Physica Scripta. Vol. 53, 76–82, 1996

Computation of the Optical Constants of Thermally-evaporated Thin Films of $GeSe_2$ Chalcogenide Glass from their Reflection Spectra

J. Ruiz-Pérez[a], E. Márquez[b], D. Minkov[c], J. Reyes[b], J. B. Ramírez-Malo[b], P. Villares[b] and R. Jiménez-Garay[b]

[a] Real Observatorio Astronómico de la Armada, 11100-San Fernando, Cádiz (Spain)[1].
[b] Departamento de Física de la Materia Condensada, Facultad de Ciencias, Universidad de Cádiz, Apdo. 40, 11510-Puerto Real, Cádiz (Spain).
[c] Department of Electronic Engineering, University of Natal, Durban (South Africa).

Received May 2, 1995; accepted July 21, 1995

Abstract

The interference modulated reflection spectra $R(\lambda)$ at normal incidence for amorphous $GeSe_2$ semiconducting films, deposited by thermal evaporation, were obtained in the spectral region from 400 nm to 2200 nm. The straightforward method proposed by Minkov, which is based on the use of the extrema of the interference fringes $R(\lambda)$, has been applied in order to obtain both the real and imaginary parts of the complex refractive index, n and k, respectively, and the film thickness, d. Thickness measurements made by a surface-profiling stylus have also been carried out to cross-check the results obtained by the optical method. The dispersion of n is discussed in terms of the single-oscillator Wemple–DiDomenico model.

1. Introduction

The excellent transmittance of chalcogenide amorphous semiconductors [1], reaching to the far-infrared spectral region, and the wide range of photo-induced effects that they exhibit (such as photo-crystallization, photo-polymerization, photo-decomposition, photo-vaporization, photo-dissolution of certain metals and photo-vitrification [2, 3]), generally accompanied by changes in the optical constants [4, 5] and, particularly shifts in the absorption edge (i.e., photo-darkening or photo-bleaching), allow their use as absorption filters and other optical elements [6]. Of these effects, metal-photodissolution (particularly, Ag-photodissolution) is probably the most useful as far as technological applications are concerned, because it produces the largest change in the optical properties of chalcogenide glasses. In addition, because of the high value of the refractive index of many crystalline materials employed in IR optics, it is necessary to coat their surface with a suitable thin film in order to reduce the reflectance [7, 8]. Since by varying the chemical composition, the refractive index of chalcogenide glasses can continuously be changed from a value of about 2.0 to 3.5 [9–13], films of these glassy materials can efficiently be used as anti-reflection coatings. The knowledge of the optical properties of chalcogenide amorphous semiconductors is, indeed, necessary for exploiting their technological potential.

The refractive index, n, and extinction coefficient, k, are usually calculated by sophisticated computer iteration techniques [14–17], using both optical transmission and reflection spectra. In contrast, a simple, straightforward method for determining the optical constants, using only the reflection spectrum, has been proposed by Minkov [18]. Using this optical method, the author has calculated the thickness, refractive index and extinction coefficient of a chalcogenide glass thin film of chemical composition $Ge_{19}As_{21}S_{60}$ attaining 1% accuracy, which is superior to the accuracy achieved by the sophisticated iteration procedures.

In this paper the Minkov's method has been used to calculate the optical constants and the thickness of thermally-evaporated thin films of the stoichiometric glassy composition $GeSe_2$.

2. Experimental details

Thin-film samples were prepared by vacuum evaporation of powdered melt-quenched glassy material onto clean glass substrates (glass microscope slides). The thermal evaporation process was performed within a coating system (Edwards, model E306A) at a pressure of about 10^{-6} Torr, using a suitable quartz crucible. During the deposition process the substrates were kept at approximately room temperature. The substrates were also rotated during the deposition process by means of a rotary workholder at a speed of ≈ 45 rpm, which makes it possible to obtain deposited $GeSe_2$ glass films of uniform thickness [19]. The deposition rate was $\approx 5\,\text{Å}\,s^{-1}$, and it was continuously measured by a quartz-crystal monitor (Edwards, model FTM-5). The low deposition rate results in a film composition which is very close to that of the bulk starting material (electron microprobe analysis has indicated that the film stoichiometry is correct to ± 0.5 at.%). The thickness of the as-deposited $GeSe_2$ glass films studied ranged between 500 nm and 1500 nm, although some thicker films were also prepared.

The reflection spectra were obtained using a double-beam UV/VIS/NIR spectrophotometer with automatic computer data acquisition (Perkin–Elmer, model Lambda-19), and the wavelength range analyzed was between 400 nm and 2200 nm. The reflection measurements were carried out against an accurately calibrated front-surfaced aluminium mirror coated with magnesium fluoride, which was taken as a reference. Since the absolute reflectance of the mirror is known in the spectral region from 400 nm to 2200 nm, data provided from the UV/VIS/NIR spectrophotometer can be transformed to absolute reflectance. The reflection measurements were made in various parts of the glass film, scanning

[1] e-mail address: ruizperez@czv1.uca.es

the entire sample, and a good reproduction of the reflection spectrum was generally achieved. The spectrophotometer was set with a slit width of 1 nm. A surface-profiling stylus (Sloan, model Dektak 3030) was also used to measure the film thickness which was compared with the thickness calculated from the reflection spectrum.

The degree of surface roughness and thickness uniformity of the $GeSe_2$ glass thin films was checked by performing some additional optical measurements, and in order to do them, the double-beam spectrophotometer was fitted with a 60 mm integrating sphere, permitting measurements from 200 nm to 2500 nm, in order to obtain the total and diffuse reflectance. These measurements have proven that the diffuse reflectance is negligibly small, and as a result, all the measured reflectance is obtained from its specular component. This means that the thin-film samples are uniform and have very smooth surfaces, and also that the theory accounting for the specular reflectance, can be properly applied. All optical measurements reported were performed at room temperature.

3. Preliminary theoretical considerations

A sketch of the optical system investigated is given in Fig. 1, showing that the reflection measurement is performed at normal incidence onto a $GeSe_2$ glass thin film evaporated onto a thick, finite and transparent substrate. The thickness of the substrate is several orders of magnitude larger than d and its refractive index is symbolized by n_s. The film is considered to be homogeneous with a constant thickness d and a complex refractive index $n_c = n - ik$, where the extinction coefficient k can be expressed by the absorption coefficient α by the equation: $k = \alpha\lambda/4\pi$. Interference effects in the thin film give rise to oscillating reflectance curves similar to those in Fig. 2, which shows two typical optical reflection spectra of $GeSe_2$ thin films having two different thicknesses. These interference fringes are used to calculate the optical constants and the thickness of the glass films, as described below.

The reflectance $R(\lambda, n_s, n, d, k)$ of the optical system shown in Fig. 1 is a complicated function [20]; the expression for R, according to Minkov [18], has the following form:

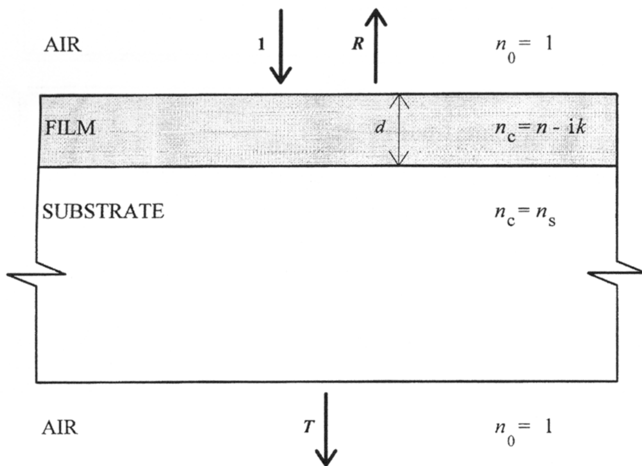

Fig. 1. Diagram showing the transmission and reflection for normal incidence onto the surface of a thin homogeneous layer of thickness d, refractive index n and extinction coefficient k on a transparent substrate (glass microscope slide) of refractive index n_s.

$$R = \frac{A' - (B_1' \cos(\varphi) - B_2' \sin(\varphi))x + C'x^2}{A'' - (B_1'' \cos(\varphi) - B_2'' \sin(\varphi))x + C''x^2} + \frac{A'''x^2}{A'' - (B_1'' \cos(\varphi) - B_2'' \sin(\varphi))x + C''x^2} \times \frac{1}{D'' - (E_1'' \cos(\varphi) - E_2'' \sin(\varphi))x + F''x^2} \quad (1)$$

where:

$$A' = [(n-1)^2 + k^2][(n+n_s)^2 + k^2], \quad (2a)$$

$$B_1' = 2[(n^2 + k^2 - 1)(n^2 + k^2 - n_s^2) + 4k^2 n_s], \quad (2b)$$

$$B_2' = 4k[n_s(n^2 + k^2 - 1) - (n^2 + k^2 - n_s^2)], \quad (2c)$$

$$C' = [(n+1)^2 + k^2][(n-n_s)^2 + k^2], \quad (2d)$$

$$A'' = [(n+1)^2 + k^2][(n+n_s)^2 + k^2)], \quad (2e)$$

$$B_1'' = 2[(n^2 + k^2 - 1)(n^2 + k^2 - n_s^2) - 4k^2 n_s], \quad (2f)$$

$$B_2'' = 4k[n_s(n^2 + k^2 - 1) + (n^2 + k^2 - n_s^2)], \quad (2g)$$

$$C'' = [(n-1)^2 + k^2][(n-n_s)^2 + k^2], \quad (2h)$$

$$A''' = 64 n_s(n_s - 1)^2(n^2 + k^2)^2, \quad (2i)$$

$$D'' = [(n+1)^2 + k^2][(n+1)(n+n_s^2) + k^2], \quad (2j)$$

$$E_1'' = 2[(n^2 + k^2 - 1)(n^2 + k^2 - n_s^2) - 2k^2(n_s^2 + 1)], \quad (2k)$$

$$E_2'' = 2k[(n^2 + k^2 - n_s^2) + (n_s^2 + 1)(n^2 + k^2 - 1)], \quad (2l)$$

$$F'' = [(n-1)^2 + k^2][(n-1)(n-n_s^2) + k^2] \quad (2m)$$

and:

$$\alpha = \frac{4\pi k}{\lambda}, \quad (3a)$$

$$x = \exp(-\alpha d), \quad (3b)$$

$$\varphi = \frac{4\pi n d}{\lambda}. \quad (3c)$$

It should be mentioned that eq. (1) represents the reflectance when the interaction between the multiple reflection rays is coherent in the film and noncoherent in the substrate.

It is known that for weakly absorbing dielectric films, when the conditions $n \gg k$ and $n_s \gg k$ are met in the spectral region considered, eq. (1) is dominated by the exponential terms in x, and the contribution of k in the other terms of the expression becomes negligibly small, and k can be considered to be zero in eq. (1) [21]. This simplifies the expression for the reflectance that becomes a function of n and x only. The envelopes of the interference maxima and minima of the reflection spectrum, R_M and R_m, are derived from eq. (1) for $k = 0$ and dielectric films with $n > n_s \gg k$, when $\varphi = \pi$ and $\varphi = 0$ respectively, are substituted.

The equations for the envelopes then have the following expressions:

$$R_M, R_m = \frac{A' \pm B_1'x + C'x^2}{A'' \pm B_1''x + C''x^2} + \frac{A'''x^2}{(A'' \pm B_1''x + C''x^2)(D'' \pm E_1''x + F''x^2)} \quad (4)$$

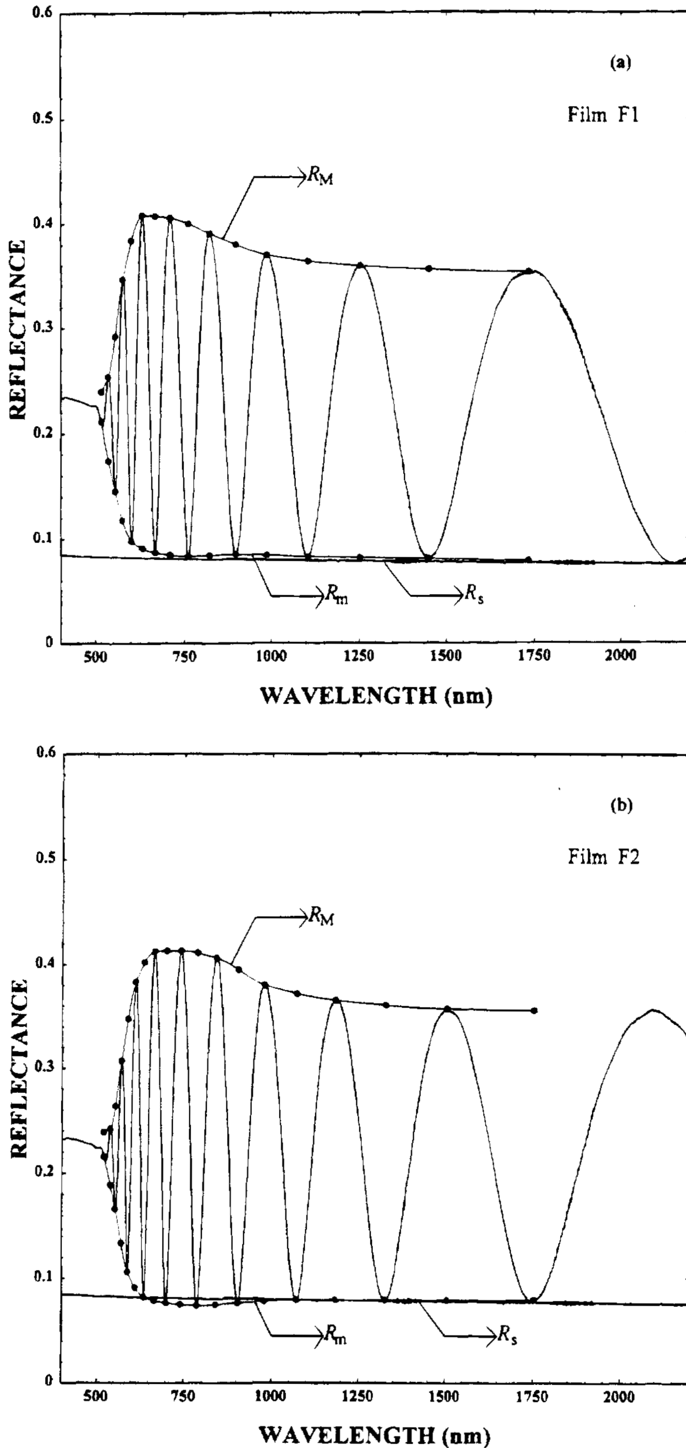

Fig. 2. Experimental optical reflection spectra corresponding to two a-$GeSe_2$ thin films ((a) film F1 and (b) film F2). Curves R_M and R_m are the maximum and minimum envelopes, respectively. R_s is the bare substrate reflection curve.

where the "+" and "−" correspond to the upper and lower envelopes, respectively, or:

$$R_M, R_m = \frac{(ad \pm bcx)^2}{(bd \pm acx)^2} + \frac{gx^2}{(bd \pm acx)^2(b^3f \pm 2abcdx + a^3ex^2)} \quad (5)$$

where $a = n - 1$, $b = n + 1$, $c = n - n_s$, $d = n + n_s$, $e = n - n_s^2$, $f = n + n_s^2$ and $g = 64n_s(n_s - 1)^2n^4$.

The refractive index of the substrate n_s is calculated from the reflection spectrum of the bare substrate R_s, with the relation:

$$R_s = \frac{(n_s - 1)^2}{n_s^2 + 1} \quad (6)$$

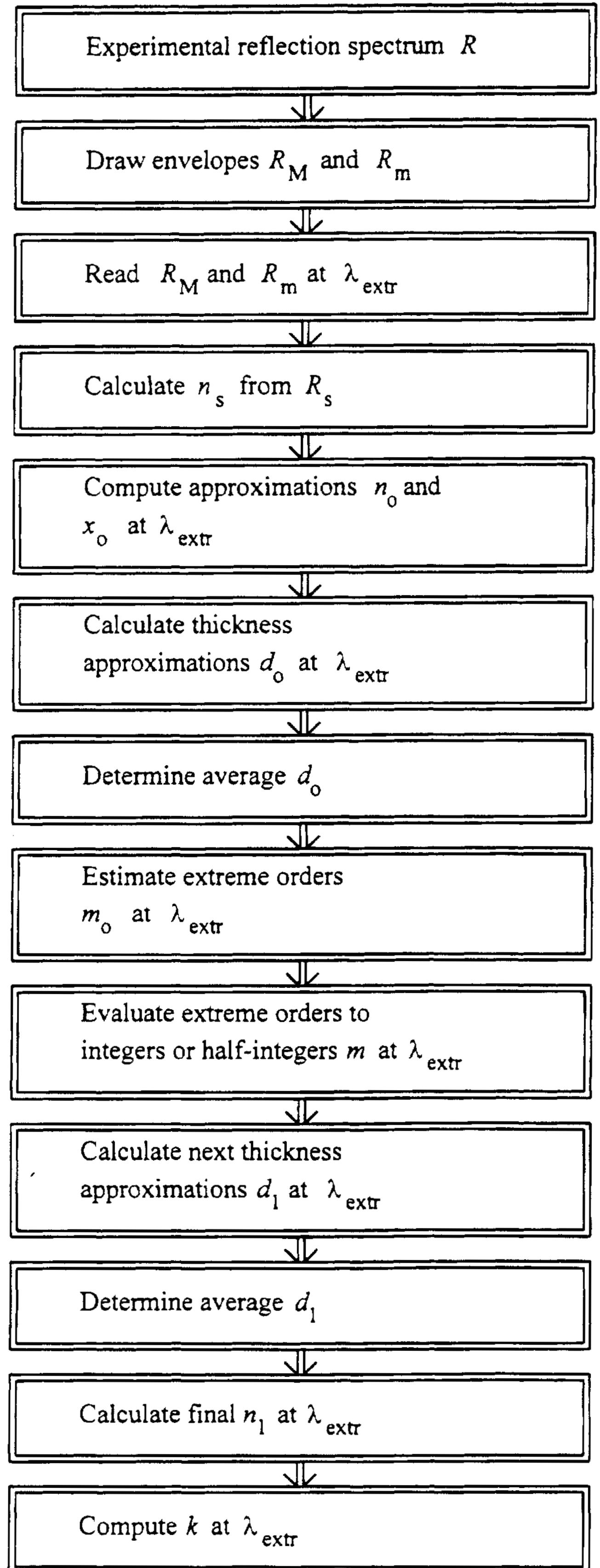

Fig. 3. Block diagram of the algorithm of the method for calculating the thickness and optical constants of a thin layer from the optical reflection spectrum only. The symbols are defined in the text at the explanation of the algorithm.

from which it is derived:

$$n_s = \frac{1 + \sqrt{R_s(2 - R_s)}}{1 - R_s}. \quad (7)$$

The block diagram of the algorithm of the method proposed by Minkov for calculating the thickness and the spectral dependencies of the refractive index and the extinction coefficient of an uniform thin film is given in Fig. 3.

4. Results and discussion

4.1. *Calculation of the refractive index and film thickness*

Following Minkov's method, the envelopes around the maxima and minima of the reflection spectrum are considered to be continuous functions of λ, and thus of $n(\lambda)$. Firstly, it is necessary to draw the envelopes R_M and R_m of the interference maxima and minima of the reflection spectrum, as shown in Fig. 2; they have been obtained using two different computer programs [22, 23], and both leading to similar results. Once the tangent points between the envelopes and the reflection spectrum λ_{extr} are known, and the refractive index of the substrate n_s is calculated from the reflection spectrum of the bare substrate R_s, the system of transcendental equations corresponding to eq. (5) is solved numerically by using the Newton–Raphson method. A distinct advantage of using the envelopes of the reflection spectrum instead of only the reflection spectrum, is that the envelopes are monotonic functions of λ, while the spectrum varies rapidly with λ. It is for this reason that the system of two equations having two unknowns has only one solution for n and x. n and x are determined as solutions of the system:

$$R_M - f_1(n, n_s, x) = 0, \quad R_m - f_2(n, n_s, x) = 0. \quad (8)$$

At every interference extreme, the solution of this system provides an initial approximation for the refractive index and absorbance of the thin film studied, n_0 and x_0, respectively, and these values are listed in Table I.

In order to calculate the initial approximation for the film thickness d, it is necessary to take into account the equation for the interference fringes:

$$2nd = m\lambda \quad (9)$$

where the order number m is an integer for the minima and half-integer for the maxima. Moreover, if n_{e1} and n_{e2} are the refractive indices at two adjacent extrema at wavelength λ_1

Table I. *Values of λ, R_M, R_m and n_s corresponding to the optical reflection spectra of Fig. 2. Calculation of d_1, n_1, k_1 and k_2 based on the present optical method; the underlined values of reflectance are the values calculated by the envelope computer program*

Sample	λ	R_M	R_m	n_s	n_0	x_0	d_0	m_0	m	d_1	n_1	k_1	k_2
F1	1734	0.353	0.079	1.500	2.373	1.0000	918	2.36	2.5	913	2.404	≈0.000	≈0.000
	1452	0.356	0.081	1.504	2.383	0.9999	921	2.83	3.0	914	2.415	≈0.000	≈0.000
	1253	0.359	0.082	1.509	2.398	0.9999	902	3.29	3.5	915	2.432	≈0.000	≈0.000
	1105	0.364	0.083	1.511	2.414	0.9999	872	3.76	4.0	916	2.451	≈0.000	≈0.000
	987	0.370	0.084	1.512	2.436	0.9999	858	4.25	4.5	912	2.463	≈0.000	≈0.000
	897	0.380	0.085	1.517	2.473	0.9999	860	4.75	5.0	907	2.487	≈0.000	≈0.000
	822	0.391	0.084	1.513	2.507	1.0000	897	5.25	5.5	902	2.507	≈0.000	≈0.000
	761	0.400	0.084	1.516	2.541	1.0001	986	5.75	6.0	899	2.532	≈0.000	≈0.000
	710	0.406	0.085	1.517	2.561	1.0000	677	6.21	6.5	901	2.559	≈0.000	≈0.000
	668	0.408	0.087	1.518	2.569	0.9999	717	6.62	7.0	910	2.593	0.0017	0.0006
	632	0.408	0.091	1.520	2.747	0.8119	1204	7.48	7.5	863	2.628	0.0038	0.0136
	602	0.384	0.098	1.521	2.735	0.7295	1454	7.82	8.0	880	2.670	0.0124	0.0181
	577	0.347	0.118	1.522	2.748	0.5652	—	8.20	8.5	893	2.720	0.0269	0.0300
	555	0.292	0.145	1.523	2.712	0.3648	—	8.41	9.0	921	2.770	0.0559	0.0460
$\bar{d}_1 = 902$ nm, $\sigma_1 = 15$ nm (1.7%)													
F2	1752	0.356	0.079	1.500	2.380	0.9999	1109	3.00	3.0	1104	2.407	≈0.000	≈0.000
	1506	0.357	0.079	1.505	2.387	1.0003	1088	3.50	3.5	1104	2.414	≈0.0000	≈0.0000
	1326	0.361	0.079	1.505	2.399	1.0000	1062	4.00	4.0	1105	2.429	≈0.000	≈0.000
	1183	0.366	0.079	1.510	2.419	0.9999	1045	4.52	4.5	1100	2.438	≈0.000	≈0.000
	1071	0.372	0.079	1.512	2.442	0.9999	976	5.04	5.0	1096	2.453	≈0.000	≈0.000
	979	0.381	0.078	1.512	2.470	1.0000	953	5.57	5.5	1090	2.466	≈0.000	≈0.000
	903	0.395	0.076	1.514	2.522	1.0000	1027	6.17	6.0	1074	2.481	≈0.000	≈0.000
	840	0.406	0.075	1.513	2.560	0.9999	1120	6.73	6.5	1066	2.501	≈0.000	≈0.000
	786	0.411	0.074	1.514	2.577	1.0000	1203	7.24	7.0	1067	2.520	≈0.000	≈0.000
	740	0.413	0.075	1.516	2.586	1.0000	1288	7.72	7.5	1073	2.542	≈0.000	≈0.000
	700	0.413	0.076	1.517	2.586	0.9999	1410	8.16	8.0	1083	2.565	≈0.000	≈0.000
	666	0.412	0.079	1.518	2.586	0.9999	1048	8.57	8.5	1095	2.593	≈0.000	≈0.000
	636	0.402	0.082	1.519	2.575	0.9698	1022	8.94	9.0	1111	2.622	0.0040	0.0012
	611	0.384	0.091	1.521	2.664	0.7956	1302	9.63	9.5	1090	2.658	0.00099	0.0103
	589	0.348	0.106	1.522	2.673	0.6358	1356	10.02	10.0	1102	2.698	0.0210	0.0189
	570	0.307	0.134	1.522	2.704	0.4355	—	10.47	10.5	1107	2.741	0.0376	0.0330
	552	0.264	0.166	1.525	2.709	0.2410	—	10.84	11.0	1121	2.781	0.0672	0.0515
$\bar{d}_1 = 1092$ nm, $\sigma_1 = 14$ nm (1.3%)													

and λ_2, respectively, the expression for the approximate thickness at every extremum is:

$$d = \frac{\lambda_1 \lambda_2}{4(\lambda_1 n_{e2} - \lambda_2 n_{e1})} \quad (10)$$

where the refractive index is assumed to be constant between λ_1 and λ_2. The values of d determined by this equation are listed as d_0 in Table I. The last few values, corresponding to the lowest wavelengths usually deviate considerably from the other values and must consequently be missed. Furthermore, the average value of d_0 corresponding to the films studied is 861 ± 90 nm and 1104 ± 123 nm for F1 and F2, respectively. The average value of d_0 is used together with n_0, in eq. (9), to calculate the "order number" m_0 for the different extrema. The accuracy of the thickness d is significantly increased by taking the corresponding exact integer or half-integer values of m associated with each extremum point, and deriving a new thickness, d_1, from eq. (9), again using the n_0-values. The values of d_1, m_0 and m for both films are also listed in Table I. The new values for the thickness d_1 have a smaller dispersion and its average value is taken as the final thickness of the film. The average thickness established for the two $GeSe_2$ glass films studied are, respectively, 902 ± 15 nm and 1092 ± 14 nm, for F1 and F2. In addition, the film thickness determined by mechanical measurements on the same film area was 913 ± 18 nm and 1080 ± 22 nm, respectively, for F1 and F2. The thickness obtained by mechanical measurements is in excellent agreement with the thickness calculated by the optical method – the difference for both films being less than 2%.

Using the accurate values of m and the average value of d_1, eq. (9) is solved for n at each λ_{extr} and, thus, the final values of the refractive index n_1 are obtained (these values are listed in Table I). The values of n_1 can be fitted to an appropriate function such as the Wemple–DiDomenico dispersion relationship [24], i.e. to the single-oscillator model:

$$\varepsilon_1(\nu) = n^2(\nu) = 1 + \frac{E_0 E_d}{E_0^2 - (h\nu)^2} \quad (11)$$

where E_0 is the energy of the effective dispersion oscillator (typically near the main peak of the ε_2-spectrum), which is identified by the mean transition energy from the valence band of the lone-pair state to the conduction-band state (in these amorphous materials, the valence s states lie far below the top of the valence-band, and the valence band edge involves transitions between lone-pair p states and antibonding conduction-band states [24]), and E_d is the dispersion energy. The oscillator energy, E_0, is an "average" energy gap, and in close approximation, it scales with the optical bandgap E_g^{opt}, $E_0 \approx 2E_g^{opt}$, as it was found by Tanaka [25]. The dispersion energy or oscillator strength, E_d, also follows a simple empirical relationship: $E_d = \beta N_c Z_a N_e$, where β is a constant, and according to Wemple [24], for covalent crystalline and amorphous materials has an empirical value of 0.37 ± 0.04 eV. N_c is the number of nearest neighbour cations to the anion, Z_a is the formal chemical valency of the anion, and N_e is the effective number of valence electrons per anion. By plotting $(n^2 - 1)$ against E^2 and fitting a straight line, E_0 and E_d can be determined directly from the slope, $(E_0 E_d)^{-1}$, and the intercept on the vertical axis, (E_0/E_d). The straight line equation corresponding to the least-squares fit, is $(n^2 - 1)^{-1} = 0.217 - 0.0128\ E^2$, with a correlation coefficient of 0.996, where the two sets of points for the two $GeSe_2$ glass thin films studied have been included. The values obtained for the dispersion parameters E_0 and E_d, derived from the above-mentioned equation, are $E_0 = 4.12$ eV and $E_d = 18.97$ eV. The Wemple–DiDomenico dispersion curve for both glass thin films, as well as the corresponding linear fit, are shown in Fig. 4, along with the calculated values for the refractive index.

Returning to the above-mentioned empirical expression for the dispersion energy E_d found by Wemple, and using the value derived for the chalcogenide glass composition studied, the value of the coordination number N_c is obtained using the relationship: $N_c = E_d/\beta Z_a N_e$, where $N_e = 8$ and $Z_a = 2$ and then N_c is ≈ 3.2. A value of the optical bandgap is also deduced from the Wemple–DiDomenico dispersion relationship, according to the expression $E_g^{opt} \approx E_0/2$, obtaining $E_g^{opt} \approx 2.06$ eV.

A simple, complementary graphical method for deriving the values of the first order number m_1 and the thickness d, based on eq. (9), is also used. This expression can be rewritten for that purpose as:

$$\frac{l}{2} = 2d\frac{n}{\lambda} - m_1 \quad (12)$$

where $l = 0, 1, 2, \ldots$. Therefore, plotting $l/2$ against n/λ yields a straight line with slope $2d$ and a cut-off on the y-axis of $-m_1$. Figure 5 displays this graph for F1 and F2, as well as the results obtained from the least-squares fit. From this plot, the values for the first order number, m_1, are obtained, being 2.38 for F1 and 3.09 for F2 (the correlation coefficients are 0.998 and 0.9990, respectively). The values of d derived from the two slopes are 882 nm and 1008 nm, respectively, in agreement with the already calculated values of $\bar{d}_1$. The differences between the two optical methods are

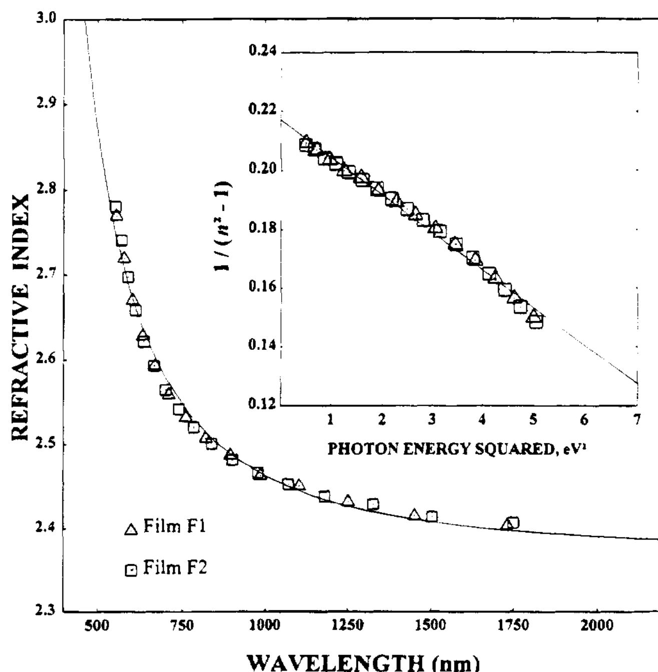

Fig. 4. Refractive index of thermally-evaporated a-$GeSe_2$ thin films versus wavelength, and the least-squares fit to the Wemple–DiDomenico dispersion relationship; in the inset, a plot of the factor $(n^2 - 1)^{-1}$ versus the photon energy squared E^2.

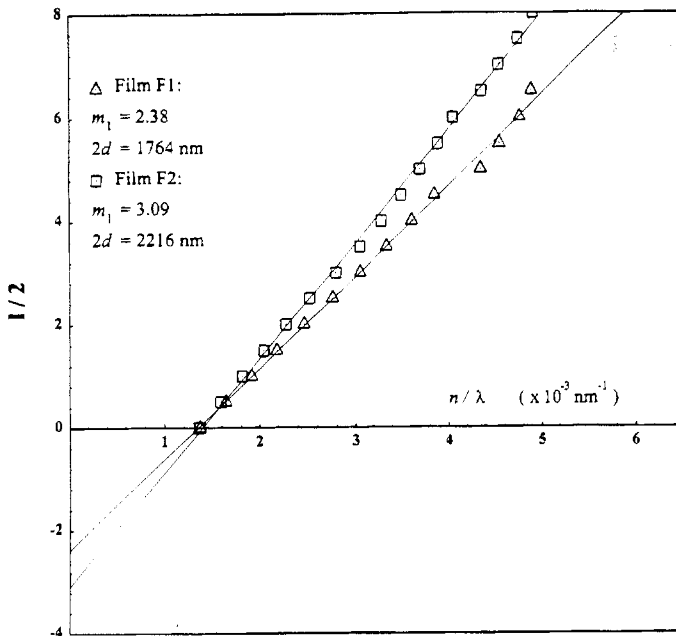

Fig. 5. Plot of $l/2$ against n/λ to calculate the first order number and film thickness for the thin-film samples F1 and F2.

about 2% which shows the significant accuracy in the calculation of $\bar{d}_1$. This graphical procedure is certainly advantageous: in principle only the values of λ and n of two interference extrema are necessary to calculate the first order number m_1 and the thickness d.

4.2. *Determination of the extinction coefficient*

The absorbance, x, is derived by numerically solving either of the two expressions for the envelopes corresponding to eq. (5); it is possible to independently solve both equations for x, thereby obtaining two different values for the absorbance, x_1 and x_2. In addition, since x and d are already known, the absorption coefficient α can be obtained from eq. (3b). The extinction coefficient, k, can then be calculated from eq. (3a). The results of the calculation of k from the envelopes R_M and R_m of the reflection spectra, are shown in Table I (the two values are listed as k_1 and k_2). The results obtained from the envelope R_M are found to be superior and this can be attributed to the fact that R_m is almost independent of n and k in the region of weak absorption, where $x \approx 1$. Moreover, in the region of transparency where $x = 1$, $R_m = R_s$, and it is seen from eq. (6) that R_m is independent of n and k. The accuracy achieved in the calculation of n in the entire spectral range is superior to that in the calculation of k in the region of medium and strong absorption, where $x < 0.9$, which is related to the stronger sensitivity of R towards changes in n than in k. Furthermore, the considerable inaccuracy in the calculation of k in the region of weak absorption is due mainly to the smaller value of k in this spectral region.

5. Concluding remarks

The method proposed by Minkov for calculating the film thickness and optical constants using only the reflection spectrum, has been successfully applied to thermally-evaporated $GeSe_2$ glass films with thicknesses ranging between 500 nm and 1500 nm. The assumptions made in the method are: both the thin film and the substrate are uniform and homogeneous, the film is absorbing and the substrate is transparent, and the interaction between the multiple reflection rays is coherent in the film and non-coherent in the substrate [20, 21, 26]. The method is applied for air as a surrounding medium with refractive index $n_0 = 1$, and the refractive index of the substrate is assumed to be dependent on the wavelength $n_s(\lambda)$.

The accuracy of the results is confirmed by comparing the experimental reflection spectrum shown in Fig. 2(a), corresponding to the sample F1, with the simulated reflection spectrum obtained by substituting the calculated film thickness and optical constants into the expression for the reflectance at normal incidence onto the film, given in eq. (1). Figure 6 shows the results in the spectral range from 500 nm to 900 nm. The excellent agreement between both reflection spectra is a consequence of the remarkably uniform thickness of the thin films, attained by using the rotary work-holder (the variation in film thickness over the area of illumination measured by the mechanical stylus, was found to be lower than ≈ 10 nm). Finally, it has to be pointed out that a lack of homogeneity in the chemical composition or of uniformity in the thickness of the thin films has a large influence on the optical reflection spectrum. If either of these drawbacks is present, the optical method can lead to serious errors, and therefore should not be applied.

The value obtained for the refractive index extrapolating the Wemple–DiDomenco dispersion relationship towards the infrared spectral region agrees very well with that found by Broese *et al.* [27] at $\lambda = 10\,\mu$m for the $GeSe_2$ glass, and also with that found by Butterfield [28] in the spectral region ranging from 600 nm to 5000 nm for the Ge–Se glass system (differences around 2% have been found in both cases). In addition, an extrapolation of the refractive index to $E = 0$ has also been performed using the Wemple–

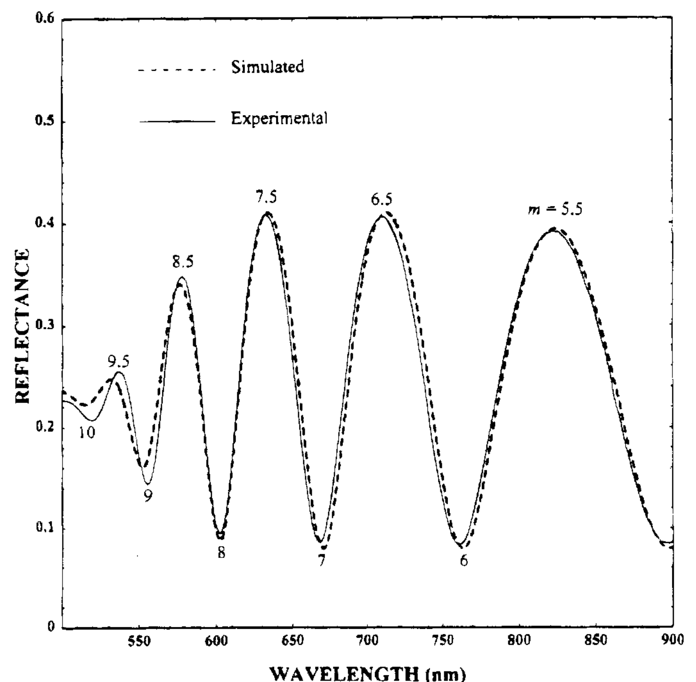

Fig. 6. Experimental optical reflection spectrum corresponding to film F1 and the simulated optical reflection spectrum, the latter obtained from the calculated value of the thickness, d = 902 nm, and the optical constants $n(\lambda)$ and $k(\lambda)$.

DiDomenico relationship, obtaining $n(0) = 2.370$, showing an excellent agreement with the value given by Kandil [29] for the present glass composition (a difference of around 3% was found).

To summarize, the method proposed by Minkov for using only the reflection spectrum to calculate d, $n(\lambda)$ and $k(\lambda)$ has proved to be useful and accurate in the case of amorphous $GeSe_2$ semiconducting films as long as they have uniform thickness. It is also worth mentioning that this method has also successfully been applied to some glassy compositions belonging to the As–S and As–Se chalcogenide binary systems obtaining very accurate results that will be published elsewhere.

Acknowledgements

The authors are grateful to Dr. I. Mártil and Dr. M. Catalán for many valuable discussions. The present work has been financially supported by grants from the Spanish Ministry of Education and Science.

References

1. Savage, J. A., "Infrared Optical Materials and Their Antireflection Coatings" (Adam Hilger, Bristol 1985).
2. Márquez, E., Jiménez-Garay, R., Zakery, A., Ewen, P. J. S. and Owen, A. E., Phil. Mag. B, **63**, 1169 (1991).
3. Márquez, E. *et al.*, Mat. Lett. **20**, 183 (1994).
4. Márquez, E. *et al.*, J. Non-Cryst. Solids **164–166**, 1223 (1993).
5. Márquez, E. *et al.*, Opt. Mater. **2**, 143 (1993).
6. Tauc, J., "Amorphous and Liquid Semiconductors" (Plenum Press, New York 1974).
7. Cox, I. T., Hass, G. and Jacobus, G. F., J. Opt. Soc. Am. **51**, 1959 (1961).
8. Cimpl, Z. and Kosek, F., J. Non-Cryst. Solids **90**, 577 (1987).
9. Rodney, W. M., Malitson, J. H. and King, K. A., J. Opt. Soc. Am. **48**, 633 (1958).
10. Hilton, A. R., Jones, C. E. and Brau, M., Phys. Chem. Glasses **7**, 105 (1966).
11. Young, P. A., J. Phys C: Solid State Phys. **4**, 93 (1971).
12. Cimpl, Z. and Kosek, F., Phys. Status Solidi (a) **93**, K55 (1986).
13. Minkov, D. A., Vateva, E., Skordeva, E., Arsova, D. and Nikiforova, M., J. Non-Cryst. Solids **90**, 481 (1987).
14. Lyashenko, S. P. and Miloslavskii, V. K., Opt. Spectrosc. **16**, 80 (1964).
15. Wales, J., Lovitt, G. J. and Hill, R. A., Thin Solid Films **1**, 137 (1967).
16. Szcyrbrowski, J. and Czapla, A., Thin Solid Films **46**, 127 (1977).
17. Vriens, L. and Rippens, W., Appl. Opt. **22**, 4105 (1983).
18. Minkov, D. A., J. Phys. D: Appl. Phys. **22**, 1157 (1989).
19. Behrndt, K. H., "Physics of Thin Films" (Academic Press, New York 1964), p. 46.
20. Heavens, O. S., "Optical Properties of Thin Solid Films" (Butterworths, London 1955), p. 74.
21. Swanepoel, R., S. Afr. J. Phys. **12**, 148 (1989).
22. McClain, M., Feldman, A., Kahaner, D. and Ying, X., Comput. Phys. **5**, 45 (1991).
23. Minkov, D. and Swanepoel, R., Optical Engineering **32**, 3333 (1993).
24. Wemple, S. H., Phys. Rev. B, **8**, 3767 (1973).
25. Tanaka, K., Thin Solid Films **66**, 271 (1980).
26. Azzam, R. M. A. and Bashara, N. M., "Ellipsometry and Polarized Light" (North-Holland, Amsterdam 1977).
27. Broese, E., Schröter, B., Lehmann, A., Richter, W. and Schirmer, G., J. Non-Cryst. Solids **130**, 52 1991).
28. Butterfield, A. W., Thin Solid Films **23**, 194 (1974).
29. Kandil, M., Ph.D. Thesis, Faculty of Science – Ain Shams University (1992).